Supplementary Data

Supplementary Figures 1-6

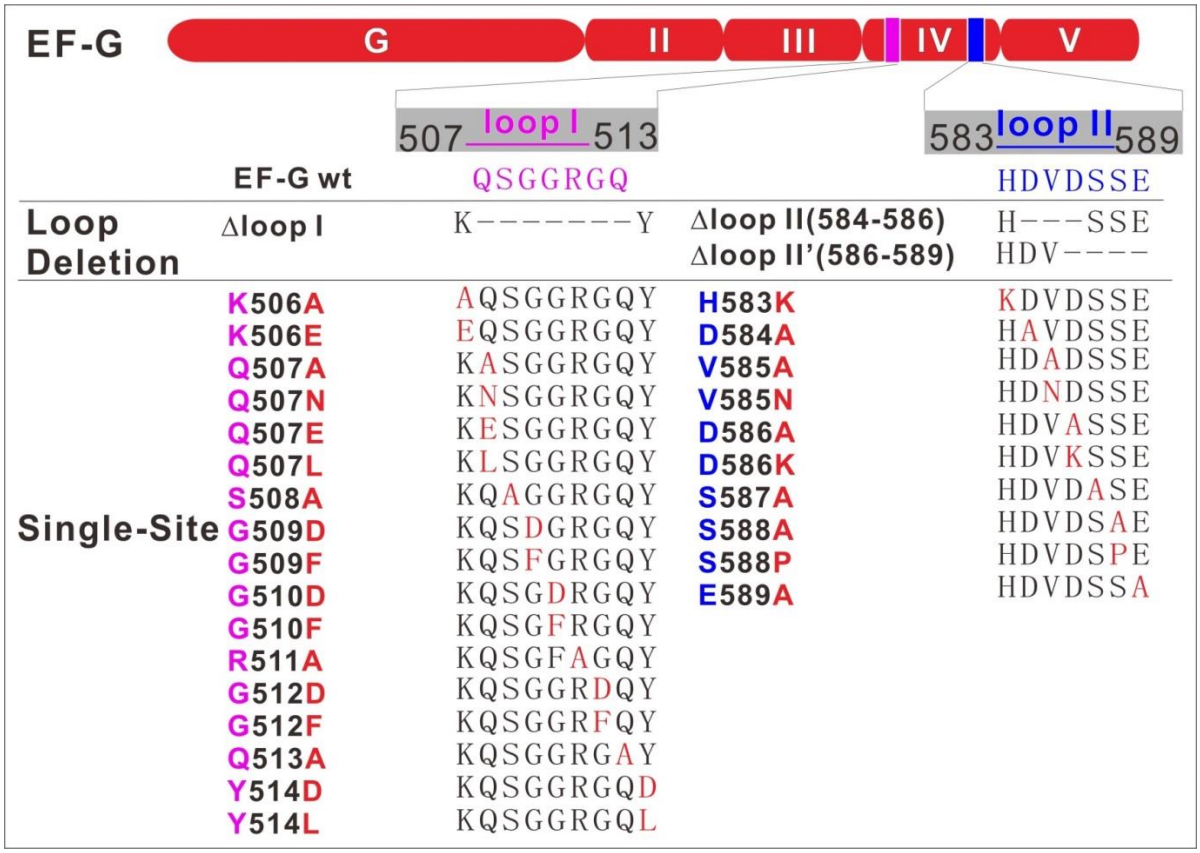

Supplementary Figure 1. Constructs of EF-G mutants in this study. The loop I and loop II of EF-G domain IV are indicated in magenta and blue, respectively. The exchanged sites are indicated in red.

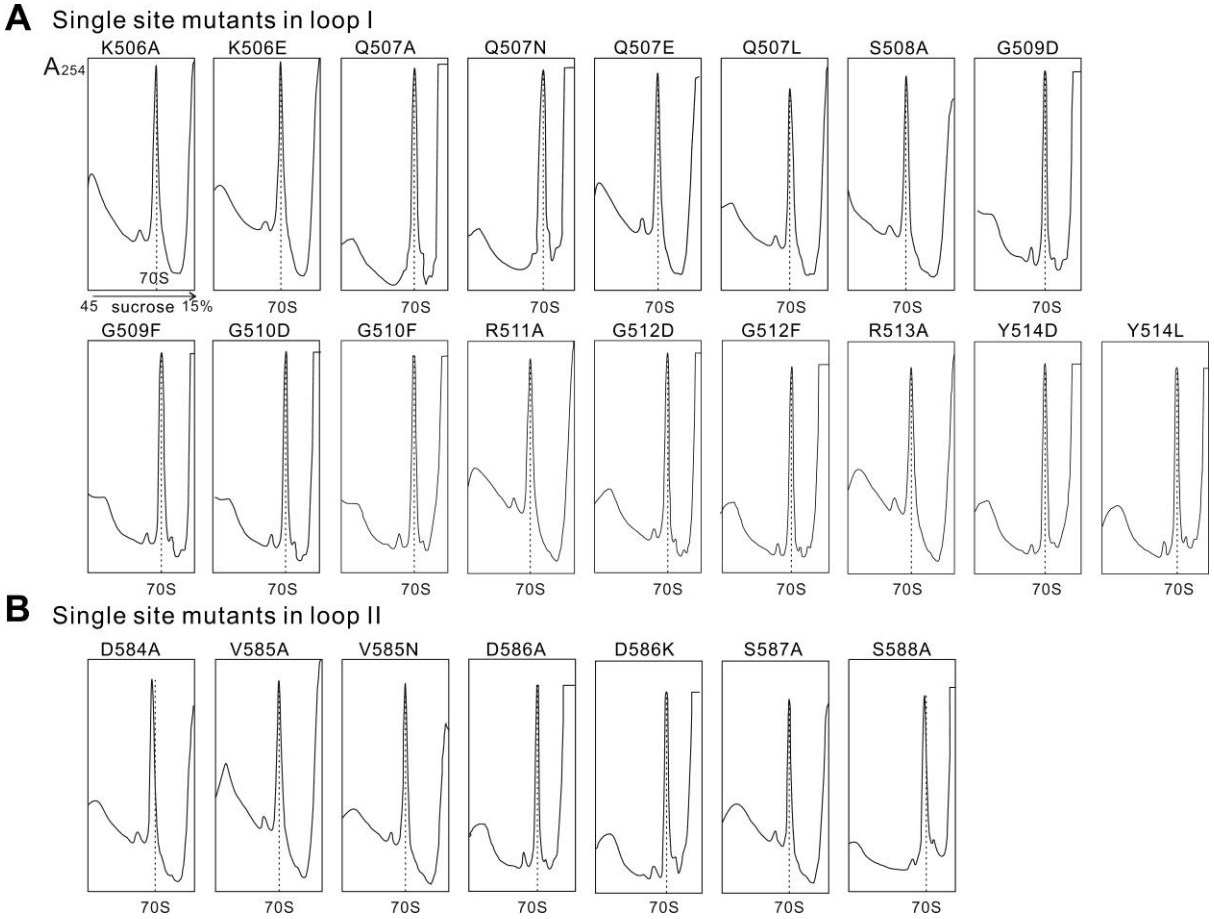

Supplementary Figure 2. The effect of EF-G single site mutants on polysome breakdown. The polysomes were incubated with RRF and EF-G mutants with single site mutation in loop I (**A**) or loops II (**B**) of domain IV. The 70S position is indicated with dashed line.

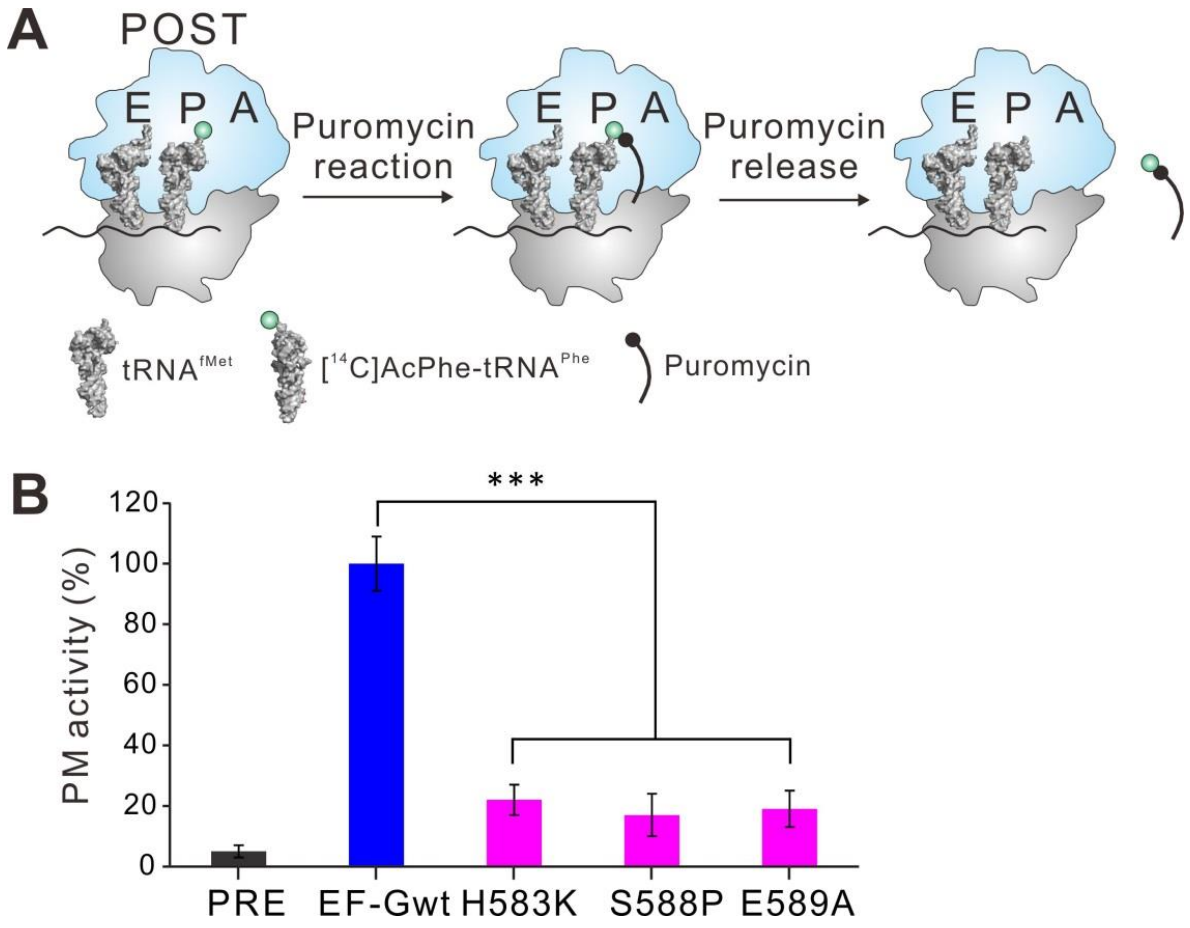

Supplementary Figure 3. The effect of EF-Gwt or mutants on puromycin (PM) activities. (**A**) Brief mechanism of PM reaction. (**B**) Effect of single site mutation on PM reactivity. Error bars, s.e.m. (n = 5 technical replicates). ****P* < 0.001.

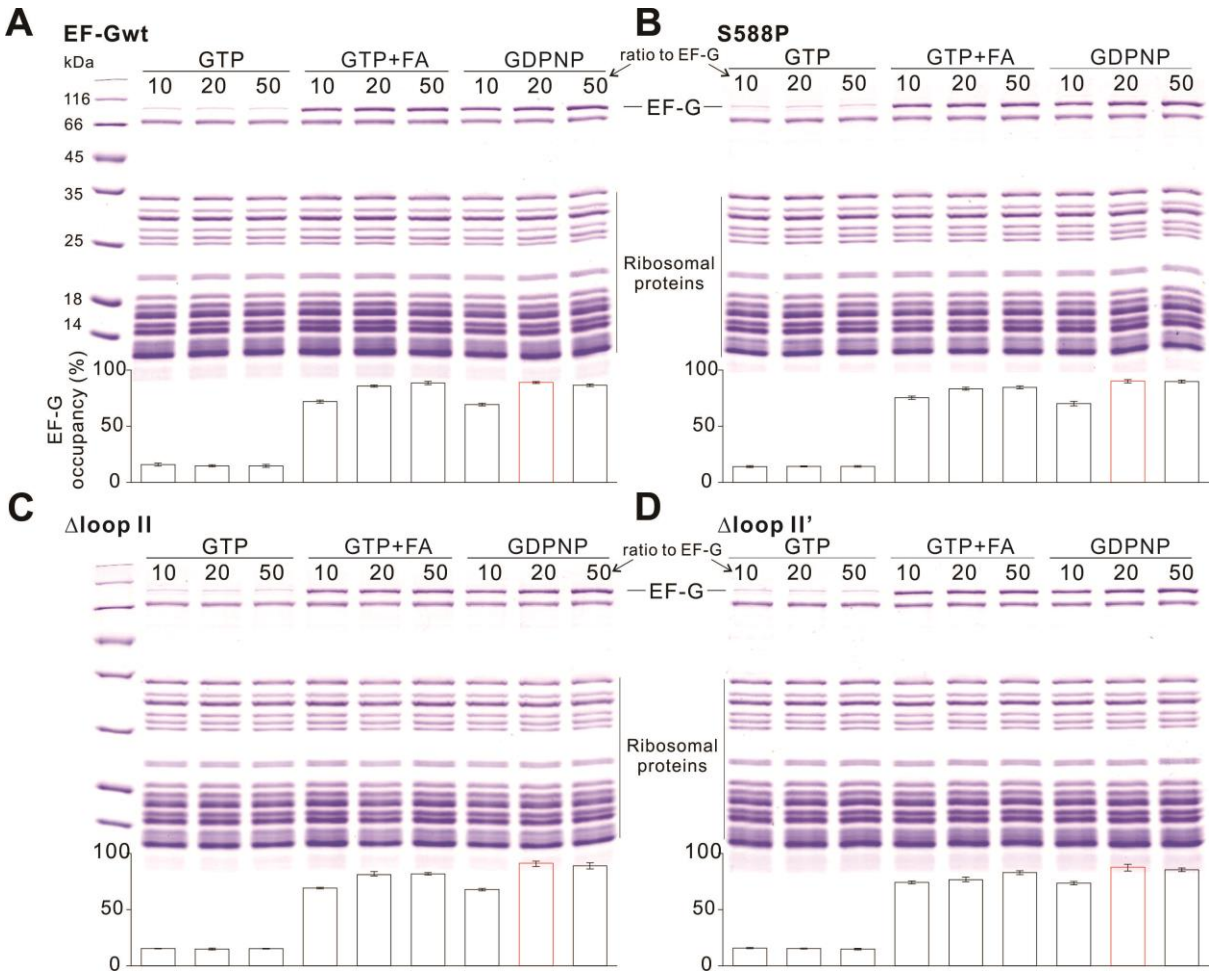

Supplementary Figure 4. Condition optimization to achieve PoTC•EF-G•RRF complex. Titration of nucleotides to EF-Gwt (**A**) or mutants (**B-D**). Quantification of EF-G occupancy on PoTC is shown beneath each gel. The optimized ratio is colored in red. Error bars, s.e.m. (n = 3 technical replicates).

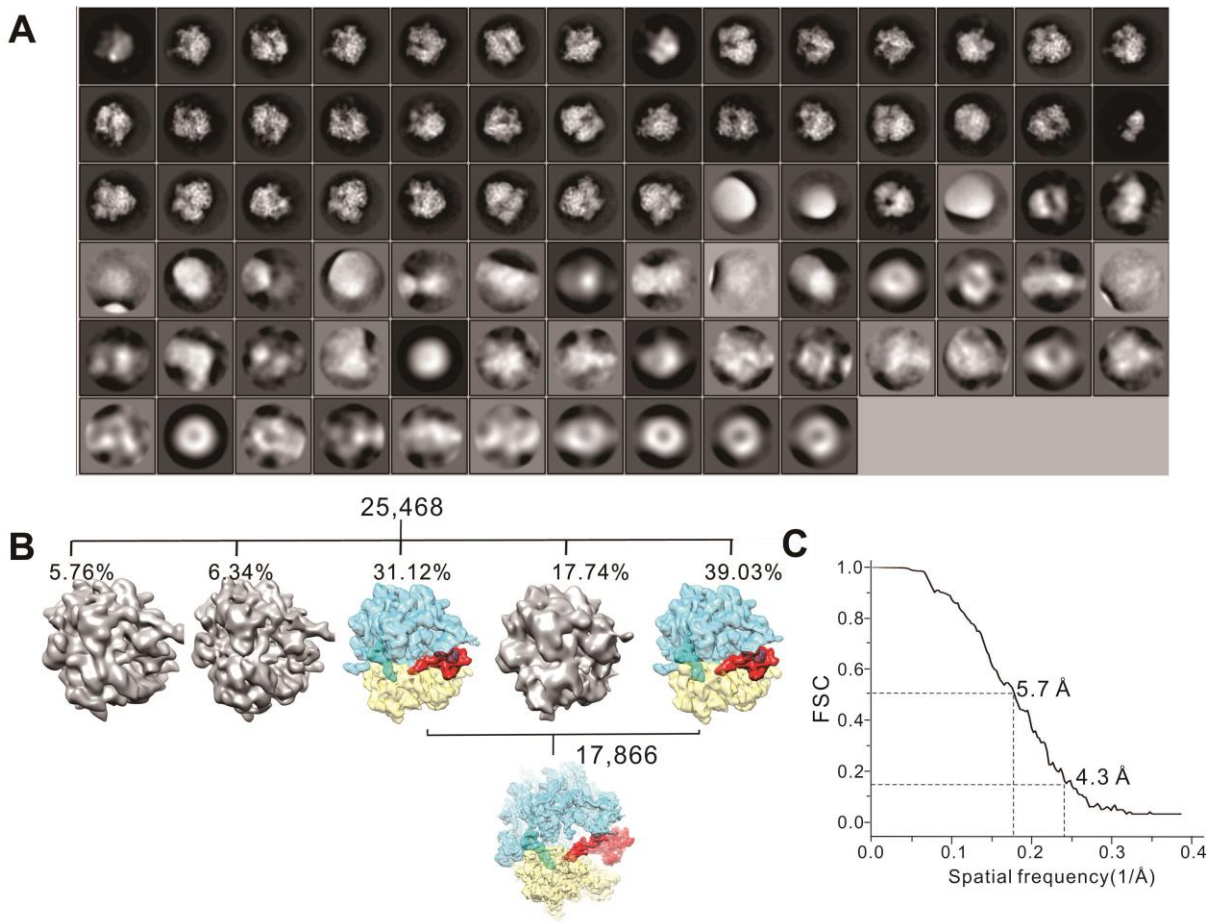

Supplementary Figure 5. (**A**) 2D class averages of cryo-EM particles. (**B**) Schematic diagram of 3D classification of PoTC•S588P•GDPNP. The detailed protocol has been described in Supplementary Methods, section of "Image processing". (**C**) Fourier Shell Correlation (FSC) curves of the PoTC complexes containing EF-G S588P mutant.

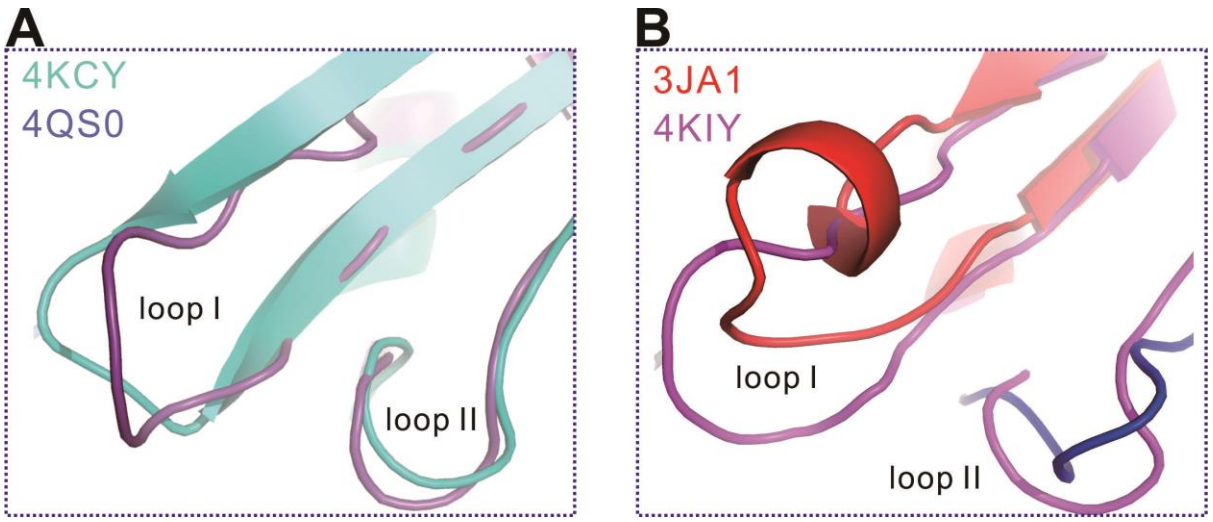

Supplementary Figure 6. Comparison of the conformations of loop I and loop II from the crystal structures of *T. thermophiles* 70S•EF-G (PDB 4KCY (1) and 4QS0 (2)) (**A**), and the cryo-EM structure of *E. coli* 70S•EF-G (PDB 3JA1 (3)) and crystal structure of *E. coli* 70S•EF-G (PDB 4KIY (4)) (**B**). Alignments were done using domain IV of EF-G as reference.

Supplementary Methods

EF-G and RRF construction and purification

All EF-G proteins used in this study were prepared according to our previous study (5). Based on the RRF gene sequence of *E. coli*, forward primer (ggaattc**catATG**ATTAGCGATATCAGAAAAGATGC) and reverse primer (ccg**ctcgag**TCAGAACTGCATCAGTTCTGCTTC) containing *NdeI* and *XhoI* restriction sites (bold underlined) respectively, were designed to amplify the *E. coli* RRF gene by PCR using genomic DNA from *E. coli* DH5*α* as the template DNA. The PCR product was inserted into the *NdeI* and *XhoI* sites of pET-22b(+) after digestion with the same enzymes, resulting in pET22b-RRF for expression of RRF with no tag. The plasmid was transformed into *E. coli* BL21 (DE3), and then RRF expression was induced with 0.5 mM IPTG at 37°C. After sonification and centrifugation, the lysate was applied to SP column. The target protein was collected and concentrated, then further purified by gel filtration with Sephadex G-75 column.

70S ribosomes, Ac-[^{14}C]-Phe-tRNA^{Phe} and mRNA preparation

Reassociated 70S ribosomes were prepared according to previously described (6). Purified $tRNA_f^{Met}$ and $tRNA^{Phe}$ from *E. coli* MRE600 were purchased from Sigma. $tRNA^{Phe}$ was aminoacylated with purified PheRS and acetylated with acetic anhydride as reported (7). MF-mRNA (5'-GGGAA GAAA**A GGAGG U**CACA U***AUGU UC***AAA GAAAA GAAAA GAAAA GAAAA GAAAA UGGAC UCAGA GCUAC GGAAA UAUUC G-3', which contains a Shine-Dalgarno sequence (bold underlined) and codes for MF (bold italic) was transcribed by T7 RNA polymerase (Promega, USA) from a double-stranded DNA template.

PoTC preparation

PoTC were prepared as described (1) with modification. Instead of MF-mRNA, here is MF-stop-mRNA with the stop codon UAA (5'-GGGAA GAAAA AAAAA UCACA U***AUGU UCUAA*** GAAAA GAAAA GAAAA GAAAA GAAAA UGGAC UCAGA GCUAC GGAAA UAUUC G-3', which contains a stop codon (bold underlined) and codes for

MF (bold italic)). Then N-Ac-Phe-tRNA^{Phe} was incorporated, followed by a puromycin treatment.

Puromycin assay

Analysis of translocation activity of EF-G was carried out according to previous studies (8,9) with minor modifications. The Pre-translocational (PRE) state complex was formed in a reaction volume of 12.5 µl containing 5 pmol 70S ribosomes, 20 pmol MF-mRNA, and 10 pmol tRNA$_f^{Met}$. The reaction mix was incubated for 15 min at 37°C to occupy the P site. The reactions were further incubated (25 µl in total) for 30 min at 37°C with 10 pmol of Ac-[^{14}C]Phe-tRNA^{Phe} to occupy the A site. For the formation of Post-translocational (POST) state complex, PRE complexes were incubated with 1 pmol EF-G in the presence of 0.1 mM GTP (35 µl in total) for the indicated time at 37°C. The puromycin reaction were performed to assess the amount of Ac-[^{14}C]Phe-tRNA^{Phe} in the P site.

***In vivo* growth assay**

LB broth was used for bacterial growth. The media was supplemented with kanamycin. IPTG was added to induce protein overexpression. The plasmids of pET-28a, *E. coli* EF-Gwt and mutants were transformed to BL21 (DE3) strain. For growth rate measurements, overnight cultures were diluted by 500-fold into 100 ml of LB medium supplemented with chemicals as indicated. The flasks (250 ml) were shaken at 200 rpm at 37°C, and 1 ml samples were collected for optical density measurements. The translation efficiency *in vivo* was analyzed by ^{35}S-methionine incorporation assay. At indicated time points, samples were taken from each culture, and the incorporation of radioactive material was determined.

Steady-state fluorescence measurements

This assay was carried out according to previous studiy (10) with minor modifications. PRE complexes were formed by activating ribosomes (0.25 µM) at 42°C for 10 min in the appropriate buffer (20 mM HEPES pH7.6, 6 mM $MgAc_2$, 150 mM NH_4Ac, 6 mM

β-Mercaptoethanol, 2 mM spermidine and 0.1 mM spermine), followed by incubation at 37°C for 10 min. Pyrene-modified mRNA (0.38 μM) was added to the ribosome and the complexes were incubated at 37°C for 6 min. Next, $tRNA_f^{Met}$ (0.3 μM) was added and the complexes were incubated at 37°C for 30 min followed by addition of Ac-[^{14}C]Phe-$tRNA^{Phe}$ (0.3 μM) and incubation at 37°C for 30 min. Steady-state fluorescence emission spectrums of PRE and POST complexes were analyzed on a Varioskan Flash Multimode Reader instrument (Thermo Scientific, USA). The PRE and POST samples were excited at 343 nm wavelength and the emission spectrum from 365–499 nm wavelengths was recorded.

Sucrose cushion assay

The experiment was prepared as described (11) with modification. Fifty pmol of 70S ribosomes were incubated with RRF, EF-G or its mutants, and guanosines in binding buffer for 15 min at 37°C in a 200 μl reaction mixture. Samples (120 μl) were overlaid onto a 75 μl sucrose cushion consisting of 1.1 M sucrose, and 25 μM guanosine in binding buffer and centrifuged at 78,000 rpm for 30 min at 4°C. The supernatant was removed, and the pellets were dissolved in 20 μl Tico buffer (20 mM HEPES-KOH pH 7.5, 6 mM $MgAc_2$, 30 mM NH_4Ac and 4 mM 2-mercaptoethanol). Five pmol ribosomes were loaded onto a 10% SDS-PAGE gel and quantified by Image-J software (NIH).

Polysomes fractionation and factor detection by western blotting

Cell lysate was layered on top of density gradient sucrose (15%-45%, w/v) in RRF buffer and centrifuged for 3.5 hr at 36,000 rpm and 4°C in a SW40 rotor. The separated samples were fractionated at 0.5 ml/min by using a fraction system monitored by A_{254} measurement. The binding of EF-G and RRF to the polysome were probed with antibodies against RRF, EF-G and S2 (Abcam, GB) and secondary mouse-anti-Rabbit antibody (Abcam). For detection, the ChemiScope 3500 Mini (CLiNX Science Instrments, CN) was used following the manufacturer's instructions.

Fluorescent labeling and FRET measurements

Mutant variants of ribosomal proteins S6 (E75C) and L9 (N11C) were created by site-directed mutagenesis, expressed, purified and labeled separately with maleimide derivatives of AF555 (donor) or AF647 (acceptor) (Lifetech, USA). Labeled proteins were used for *in vitro* reconstitution as described (12). Reconstituted 30S and 50S subunits were associated in a reaction buffer containing 20 mM HEPES pH7.6, 20 mM $MgAc_2$, 100 mM NH_4Ac, 6 mM β-Mercaptoethanol and 2 mM spermidine for 10 min at 37°C. Labeled 70S ribosomes were then isolated after centrifugation through a 10%–30% (w/v) sucrose gradient. Ribosomal complexes were constructed and all FRET measurements taken in buffer containing 20 mM HEPES pH7.6, 6 mM $MgAc_2$, 150 mM NH_4Ac, 6 mM β-Mercaptoethanol, 2 mM spermidine and 0.1 mM spermine. PoTC complexes were constructed by incubation of 70S ribosomes (0.5 μM) with MF-stop-mRNA (1 μM) and N-Ac-Phe-$tRNA^{Phe}$ (1 μM) for 20 min at 37°C. PoTC complex was treated with puromycin and diluted to a final concentration of 0.1 μM. Finally, the samples were incubated with EF-G (4 μM) and GDPNP (0.4 mM) for 10 min at 37°C. Details of the fluorescence measurements and data analysis were performed as previously described (13,14). Briefly, fluorescence measurements were taken using F-4500 FL spectrophotometer (Hitachi) at 20°C. Two emission spectra were taken for each sample by exiting fluorescence at 550 nm (emission 560-800 nm) and 640 nm (emission 650-800 nm). The slit-widths for both excitation and emission were set to 5 nm spectral bandwidth. All experiments were done at least three times.

Cryo-electron microscopy and data collection

The ribosome sample with EF-G S588P was prepared as described (5) with modification. Briefly, 10 pmol of PoTC complex, 100 pmol of EF-G S588P and 5 μmol GDPNP were incubated together for 10 min at 37°C and diluted to a final concentration of ~60 nM. An aliquot of 3.5 μl of the diluted samples was applied to a Quantifoil R2/2 200 mesh holey grid (Quantifoil Micro Tools GmbH, Jena, Germany) and blotted for 4s in a chamber at 100% humidity using an FEI Vitrobot Mark IV. Images were taken using an FEI Titan Krios cryo electron microscope equipped with a Gatan K2 camera, operated at accelerating voltage of 300kV with magnification set to 22,000x. Defocus values in the final data set ranged from 1.5 to 3.5 μm. Data

acquisition was performed using UCSF-Image4 (written by X. Li and Y. Cheng, UCSF), with a nominal magnification of 22,500 x, which yields a final pixel size of 1.32 Å at object scale, and with defocus ranging from -1.5 μm to -3.5 μm. A dose rate on the detector was about 8.2 counts per pixel per second with a total exposure time of 8 seconds. Each micrograph stack contains 32 frames.

Image processing

Beam-induced motion correction at micrograph level was done according to a published protocol to produce average microgrpahs over all frames (15). Preprocessing of micrographs (461 in total) and particle picking were performed with standard SPIDER protocols (16). Particles-picking were done using a method based on a locally normalized cross-correlation function (17). Program of CTFFIND3 (18) was used to estimate the contrast transfer function parameters. The 2D, 3D classification and refinement were performed with RELION. An initial dataset of 30,103 particles was imported into RELION (19) and subjected to reference free 2D classification (80 classes) (Supplementary Figure 5A). Good particles were combined (25,468 in total) and subjected to three dimensional (3D) classification (Supplementary Figure 5B). Particles were split into five groups. Two of them displayed well defined fine features on 3D structures, and therefore combined for structural refinement (17,866). A low-pass filtered (40 Å) empty 70S map was used as the reference during 3D classification. To minimize the reference bias, the 3D classification was done in four steps: (1) global and local search with an angular step of 7.5° for 25 iterations (5 iterations without angular restriction and 20 iterations with 60° restriction) ; (2) local search (with 37° restriction) with an angular step of 3.7° for 25 iterations; (3) local search (with 18° restriction) with an angular step of 1.8° for 25 iterations; (4) local search (with 9° restriction) with an angular step of 0.9° for 25 iterations. Structural refinement was done with a new set of dose-reduced particles only containing information from frames 3-14. Resolution estimations were done using the gold-standard FSC procedure, with a soft mask applied (Supplementary Figure 5C). Chimera (20) was used for structural analysis and figure preparation.

Supplementary References

1. Zhou, J., Lancaster, L., Donohue, J.P. and Noller, H.F. (2013) Crystal structures of EF-G-ribosome complexes trapped in intermediate states of translocation. *Science*, **340**, 1236086.
2. Zhou, J., Lancaster, L., Donohue, J.P. and Noller, H.F. (2014) How the ribosome hands the A-site tRNA to the P site during EF-G-catalyzed translocation. *Science*, **345**, 1188-1191.
3. Li, W., Liu, Z., Koripella, R.K., Langlois, R., Sanyal, S. and Frank, J. (2015) Activation of GTP hydrolysis in mRNA-tRNA translocation by elongation factor G. *Science advances*, **1,** e1500169.
4. Pulk, A. and Cate, J.H. (2013) Control of ribosomal subunit rotation by elongation factor G. *Science*, **340**, 1235970.
5. Liu, G., Song, G., Zhang, D., Zhang, D., Li, Z., Lyu, Z., Dong, J., Achenbach, J., Gong, W., Zhao, X.S. *et al.* (2014) EF-G catalyzes tRNA translocation by disrupting interactions between decoding center and codon-anticodon duplex. *Nat. Struct. Mol. Biol.* , **21**, 817-824.
6. Blaha, G., Stelzl, U., Spahn, C.M., Agrawal, R.K., Frank, J. and Nierhaus, K.H. (2000) Preparation of functional ribosomal complexes and effect of buffer conditions on tRNA positions observed by cryoelectron microscopy. *Methods Enzymol.* , **317**, 292-309.
7. Walker, S.E., Shoji, S., Pan, D., Cooperman, B.S. and Fredrick, K. (2008) Role of hybrid tRNA-binding states in ribosomal translocation. *Proc Natl Acad Sci U S A*, **105**, 9192-9197.
8. Dinos, G., Kalpaxis, D.L., Wilson, D.N. and Nierhaus, K.H. (2005) Deacylated tRNA is released from the E site upon A site occupation but before GTP is hydrolyzed by EF-Tu. *Nucleic Acids Res*, **33**, 5291-5296.
9. Watanabe, S. (1972) Interaction of siomycin with the acceptor site of Escherichia coli ribosomes. *J Mol Biol*, **67**, 443-457.
10. Studer, S.M., Feinberg, J.S. and Joseph, S. (2003) Rapid kinetic analysis of EF-G-dependent mRNA translocation in the ribosome. *J. Mol. Biol.* , **327**, 369-381.
11. Connell, S.R., Trieber, C.A., Dinos, G.P., Einfeldt, E., Taylor, D.E. and Nierhaus, K.H. (2003) Mechanism of Tet(O)-mediated tetracycline resistance. *EMBO J.* , **22**, 945-953.
12. Majumdar, Z.K., Hickerson, R., Noller, H.F. and Clegg, R.M. (2005) Measurements of internal distance changes of the 30S ribosome using FRET with multiple donor-acceptor pairs: quantitative spectroscopic methods. *J. Mol. Biol.* , **351**, 1123-1145.
13. Hickerson, R., Majumdar, Z.K., Baucom, A., Clegg, R.M. and Noller, H.F. (2005) Measurement of internal movements within the 30 S ribosomal subunit using Förster resonance energy transfer. *Journal of molecular biology*, **354**, 459-472.
14. Ermolenko, D.N., Majumdar, Z.K., Hickerson, R.P., Spiegel, P.C., Clegg, R.M. and Noller, H.F. (2007) Observation of intersubunit movement of the ribosome in solution using FRET. *J. Mol. Biol.* , **370**, 530-540.
15. Li, X., Mooney, P., Zheng, S., Booth, C.R., Braunfeld, M.B., Gubbens, S., Agard, D.A. and Cheng, Y. (2013) Electron counting and beam-induced motion correction enable near-atomic-resolution single-particle cryo-EM. *Nat. Methods* **10**, 584-590.
16. Shaikh, T.R., Gao, H., Baxter, W.T., Asturias, F.J., Boisset, N., Leith, A. and Frank, J. (2008) SPIDER image processing for single-particle reconstruction of biological macromolecules from electron micrographs. *Nat. Protoc.* , **3**, 1941-1974.
17. Rath, B.K. and Frank, J. (2004) Fast automatic particle picking from cryo-electron micrographs using a locally normalized cross-correlation function: a case study. *J. Struct. Biol.* , **145**, 84-90.
18. Mindell, J.A. and Grigorieff, N. (2003) Accurate determination of local defocus and specimen tilt in electron microscopy. *J. Struct. Biol.* , **142**, 334-347.

19. Scheres, S.H. (2012) A Bayesian view on cryo-EM structure determination. *J. Mol. Biol.* , **415**, 406-418.
20. Pettersen, E.F., Goddard, T.D., Huang, C.C., Couch, G.S., Greenblatt, D.M., Meng, E.C. and Ferrin, T.E. (2004) UCSF Chimera--a visualization system for exploratory research and analysis. *J. Comput. Chem.* , **25**, 1605-1612.